Modeling Surface Tension in SPH by Interface Reconstruction using Radial Basis Functions

Björn Andersson, Stefan Jakobsson, Andreas Mark, Fredrik Edelvik
Fraunhofer-Chalmers Centre
Chalmers Science Park
Göteborg, Sweden
{bjorn.andersson, stefan.jakobsson, andreas.mark, fredrik.edelvik}@fcc.chalmers.se

Lars Davidson
Department of Applied Mechanics
Chalmers University of Technology
Göteborg, Sweden
lars.davidson@chalmers.se

***Abstract*—A novel method for reconstructing the interface between two fluids is described and evaluated. The method uses a different basis for approximating the color function than what is common practice in SPH simulations. The key feature of the new method is the ability to omit small length scale structures in order to obtain a smoother representation. A smoother interface is more suitable to derive a surface tension force from, as the magnitude of the force is proportional to the curvature which is related to the second derivative along the interface.**

I. Introduction

At an interface between two different fluids, or a fluid and a solid wall, there is in general a surface tension associated with it. Several attempts have been made to model this effect within the framework of *Smoothed Particle Hydrodynamics* (SPH). Morris [1] describes a method where the surface tension is modeled on a macroscopic level using the curvature of the interface. Tartakovsky and Meakin [2] model the surface tension as inter-particle forces, which cancel out in the bulk of the fluid. Both methods are so-called *Continuum Surface Force* (CSF) methods [3], where the surface tension is modeled as a volume force in a narrow region close to the interface. In this way more particles than those immediately close to the interface experience the surface tension.

The method described here is similar to that of Morris in that it attempts to estimate the curvature of the interface in a macroscopic sense. The general motivation for doing so is that the surface tension force acting on a fluid element can be written

$$\boldsymbol{F}_s = \sigma\kappa\hat{\boldsymbol{n}} - \nabla_S\sigma, \tag{1}$$

where σ is surface tension coefficient, κ is the mean curvature of the interface, $\hat{\boldsymbol{n}}$ is the interface normal and ∇_S is the interface tangential differential operator. The latter term, known as the Marangoni effect, is in the following assumed to be zero and is not considered.

The surface acting as an interface between the different phases is tracked by means of a *color function*, $C(\boldsymbol{x})$. Each of the phases is assigned a different color which is propagated with the fluid. In a Lagrangian method, such as SPH, this is particularly easy as each particle is assigned a color at the start of the simulation and it is then kept at that same color throughout the simulation. The color field is then used to evaluate the surface tension. The direction of the surface tension force is evaluated as the gradient of the color function, and the strength is proportional to the second derivative along the interface. Therefore it is important to have a sufficiently smooth color function that does not vary too rapidly in space compared to the size of the SPH particles.

The standard SPH framework offers a couple of different options for discretization of the curvature and surface normals based on the color function [1], [4]. They all have in common that the length scale of the correlation of the color function is of the same order as the size of the particles. The reason for this is that the color field is determined from the particles alone, using SPH interpolation. However, the length scale of the second derivative will be much shorter, and as a result the estimate of the curvature will be strongly dependent on the particle distribution.

The remedy to this problem suggested here is to use a different basis for interpolating and/or approximating the color function. The framework chosen is *Radial Basis Function*s (RBF) [5], which shares some common features with SPH. One significant advantage of the RBF approach is the possibility to introduce a relaxation parameter that can be varied continuously, resulting in pure interpolation in one limit, and a very smooth, but crude approximation in the other limit. This parameter is then used to obtain a reconstruction of the interface having appropriate smoothness on the length scale of the SPH particle radius.

The smoothness is particularly important if the two phases solved for have a large density difference. If, for example, water droplets in air are studied, the density ratio is about 1000 to 1, and depending on the situation the air flow may have negligible influence on the water droplets. If that is the case, it is enough to solve for the denser phase, in effect treating the other as massless. This will in the following be the case; only the denser phase is treated, turning the interface into a free surface.

The outline of the paper is as follows: In Section II the governing equations and their discretization is described. Section III gives an overview of the RBF results relevant to the present work. In Section IV the reconstruction of the interface is described and the expression for the surface tension force

is stated. Section V gives some numerical results for two test cases, and Section VI concludes the paper with a discussion and some suggestions for areas where more work is needed.

II. Governing equations and Discretization

The equations to solve are the incompressible, isothermal, Navier-Stokes (N-S) equations in a moving Lagrangian frame,

$$\frac{\partial \boldsymbol{v}}{\partial t} = \frac{1}{\rho}\left[\mu\nabla^2\boldsymbol{v} + \boldsymbol{F}_s - \nabla p\right] + \boldsymbol{g} \tag{2a}$$

$$\frac{\partial \rho}{\partial t} = -\rho\nabla\cdot\boldsymbol{v} = 0, \tag{2b}$$

where $\boldsymbol{v}$ is the fluid velocity, t is time, ρ is the fluid density, μ is the dynamic viscosity, $\boldsymbol{F}_s$ is the surface tension force, p is the pressure, and $\boldsymbol{g}$ is the gravitational acceleration.

The discretization method is SPH, in which particles carry physical properties such as density, velocity and color. The color is used to track different phases, each assigned its color according to the formula,

$$C_\alpha = \alpha,$$

where α enumerates the phases. Central to the concept of SPH is interpolation among the particles, or interpolation points as they are also known as. The standard way of obtaining the value of a physical quantity at a position $\boldsymbol{x}$ in space is to evaluate the interpolation,

$$A(\boldsymbol{x}) = \sum_{j=1}^{N} A_j V_j\, W(R_j)\,,$$

where $V_j = m_j/\rho_j$ is the volume occupied by particle j, $W(\cdot)$ is the kernel function, h_j is the particle radius, $R_j = |\boldsymbol{x} - \boldsymbol{x}_j|/h_j$ the scaled distance to the particle, and A_j is the value of A at particle j.

In the present work all particles are assigned the same mass, $m_j = m$, and radius, $h_j = h$. A quintic spline kernel [6],

$$W(R) = \alpha \begin{cases} (3-R)^5 - 6\,(2-R)^5 + 15\,(1-R)^5\,, & 0 \le R < 1, \\ (3-R)^5 - 6\,(2-R)^5\,, & 1 \le R < 2, \\ (3-R)^5\,, & 2 \le R < 3, \\ 0, & R \ge 3, \end{cases}$$

with normalization $\alpha = 7/(478\pi h^2)$ in two spatial dimensions, is used in the simulations. The radius of support for this kernel is 3, which means that particles within range of $3h$ contributes when evaluating the SPH interpolation for each particle. In two spatial dimensions this amounts to about 25 other neighboring particles within the domain of support.

The N-S equations are solved as described by Cummins and Rudman [7], where the momentum equation is first solved without the pressure gradient term. An intermediate velocity field, $\boldsymbol{v}^*$, is obtained which in general is not divergence free. A pressure Poisson equation focusing on a divergence free velocity field in Eq. 2b,

$$\nabla\cdot\left(\frac{1}{\rho}\nabla p\right) = \frac{\nabla\cdot\boldsymbol{v}^*}{\Delta t},$$

where Δt is the time step, is solved which gives a pressure that projects out the divergence of the intermediate velocity. The update formula is then

$$\boldsymbol{v}^{t+\Delta t} = \boldsymbol{v}^* - \Delta t\,\frac{1}{\rho}\nabla p,$$

where $\boldsymbol{v}^{t+\Delta t}$ is the velocity field at the next time step.

The viscosity term of Eq. 2a is discretized as

$$\frac{\mu}{\rho_i}\nabla^2\boldsymbol{v}_i = \sum_{j=1}^{N} 8\mu m \frac{(\boldsymbol{v}_i - \boldsymbol{v}_j)}{(\rho_i+\rho_j)^2}\frac{(\boldsymbol{x}_i - \boldsymbol{x}_j)\cdot\nabla W(R_{ij})}{\left(|\boldsymbol{x}_i - \boldsymbol{x}_j|^2 + \zeta^2 h^2\right)},$$

assuming constant viscosity μ. The argument to the kernel function R_{ij}, is the distance between particles i and j and the term involving the small quantity ζ^2 of the order 10^{-2} in the denominator is added to avoid singularities for particles placed close together.

The pressure gradient term is evaluated as

$$\frac{1}{\rho_i}\nabla p_i = \sum_{j=1}^{N} m\left(\frac{p_i}{\rho_i^2} + \frac{p_j}{\rho_j^2}\right)\nabla W(R_{ij})\,.$$

The treatment of the surface tension force is described in section IV-B, but first some more theory has to be described.

III. Overview of Radial Basis Functions

The Radial Basis Function (RBF) framework is in some sense very similar to that of SPH. Both methods rely on interpolation points spread out in space, and they do not have to be regularly distributed on a grid. Here, only the theory needed for the application at hand is described and the reader is referred to [5], [8], [9] for a more thorough description.

A. Interpolation

At each interpolation point a radial basis function is centered, and a weight is associated to it. As in SPH, the function value at a point $\boldsymbol{x}$ is obtained by evaluating a sum over the interpolation points,

$$f(\boldsymbol{x}) \approx S(\boldsymbol{x}) = \sum_{i=1}^{N} \lambda_i \phi\left(r_i\right) + p\left(\boldsymbol{x}\right),$$

where $f(\boldsymbol{x})$ is the true function, $S(\boldsymbol{x})$ its interpolation, λ_i are the weights associated with the interpolation points, $\phi(\cdot)$, is the radial basis function, $r_i = |\boldsymbol{x} - \boldsymbol{x}_i|$ is the distance to the center of particle i located at $\boldsymbol{x}_i$, and $p\left(\boldsymbol{x}\right)$ is a low degree polynomial. The polynomial term may or may not be needed depending on the choice of ϕ. If, for example, a Gaussian is chosen, the polynomial part is not needed, but for a cubic spline, $\phi\left(r\right) = r^3$, as is used in the present work, a polynomial of degree 1 is added.

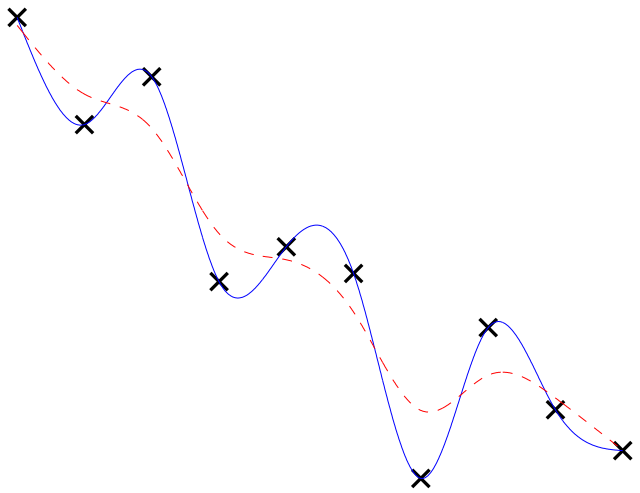

Fig. 1. Interpolation (full blue line) and approximation (dashed red line) of data points (black $\times$) corresponding to a random walk in one dimension. By approximating the data a smoother function is obtained, which still recovers the overall trend and some of the major features.

B. Approximation

Connected to each choice of ϕ is a native space, $\mathcal{N}_\phi$, equipped with a semi-norm. The RBF interpolant is the function that interpolates the data and has the minimal native space norm,

$$S = \arg \min_{\tilde{S}(\boldsymbol{x}_k)=f_k} \left|\tilde{S}\right|_{\mathcal{N}_\phi}.$$

The native space norm can be said to be a measure of bumpiness of the interpolation, which makes the above criterion to select the least bumpy interpolant of all possible choices. As comparison we mention that cubic spline interpolation results in an interpolation that minimizes the L^2-norm of the second derivative, as explained in [5, p. 9].

However, there is of course a lower limit to how smooth the interpolant can be, given the data to interpolate. To obtain an even smoother reconstruction of the data we must therefore relax the interpolation criterion and turn to approximation. If we include an error vector in the definition of the interpolation criterion,

$$S(\boldsymbol{x}_k) = f_k + e_k, \tag{3}$$

we get an approximation to the data, and the error at each point can, in some sense, be used to smooth $S(\boldsymbol{x})$. An example is shown in Fig. 1 where scattered data in one dimension is both interpolated and approximated in order to demonstrate the effect. The difference between the approximation (red dashed line in Fig. 1) and the data at each point is the error e_k.

Mathematically the approximation condition in Eq. 3 can be stated in the RBF framework as

$$S = \arg \min_{\tilde{S}(\boldsymbol{x}_k)=f_k+e_k} \eta\left|\tilde{S}\right|^2_{\mathcal{N}_\phi} + (1-\eta)\left|\boldsymbol{e}\right|^2_{l^2}.$$

Here the parameter $\eta \in (0,\, 1)$ changes from putting all the weight on the error as $\eta \to 0_+$, to only measure the native space norm as $\eta \to 1_-$. In the lower limit, the minimum $|\boldsymbol{e}|^2_{l^2} = 0$ is recovered for pure interpolation. In the upper limit the bumpiness is minimized without consideration of the error and the smoothest approximation available is obtained. If a cubic spline if chosen for $\phi(r)$ this is a polynomial of degree at most one.

A more detailed discussion on these approximation features of RBF can be found in [10].

C. Derivatives

In order to obtain derivatives of the reconstructed function the approximation is differentiated, as in SPH, and one obtains an exact derivative of an approximate function. The expressions for the gradient and Hessian are, respectively,

$$\nabla S(\boldsymbol{x}) = \sum_{i=1}^{N} \lambda_i \frac{(\boldsymbol{x}-\boldsymbol{x}_i)}{r_i}\frac{d\phi\,(r_i)}{dr} + \nabla p\,(\boldsymbol{x})\,,$$

$$H(S(\boldsymbol{x})) = \sum_{i=1}^{N} \lambda_i \left[\frac{(\boldsymbol{x}-\boldsymbol{x}_i)\otimes(\boldsymbol{x}-\boldsymbol{x}_i)}{r_i^2}\left(\frac{d^2\phi\,(r_i)}{dr^2} - \frac{1}{r_i}\frac{d\phi\,(r_i)}{dr}\right) + \frac{\boldsymbol{I}}{r_i}\frac{d\phi\,(r_i)}{dr}\right] + H(p(\boldsymbol{x}))\,,$$

where $(\cdot \otimes \cdot)$ denotes the outer product and $\boldsymbol{I}$ the identity matrix. If $p(\boldsymbol{x})$ is a linear polynomial the term $H(p(\boldsymbol{x}))$ vanishes.

If a cubic spline is chosen for ϕ, all terms in the expressions for the gradient and Hessian are bounded and otherwise well behaved, and there is reason to believe that the true derivatives of the interpolated function are well recovered for reasonably smooth interpolation data.

IV. Interface reconstruction

The interface between different phases is reconstructed by means of an implicit surface, defined as

$$\Gamma = \left\{\boldsymbol{x} \in \Omega : \tilde{C}\,(\boldsymbol{x}) = C_I\right\},$$

where $\tilde{C}\,(\boldsymbol{x})$ is the approximate color function and C_I is the mean value of the color of the two fluids on either side of the interface. $\tilde{C}$ is defined as an RBF approximation of the color function as defined by the SPH particles.

A. Approximation of the color function

In order to build the approximation, the color function is evaluated by an SPH interpolation formula on a fine grid covering the whole computational domain. The expression used to evaluate the color function is

$$C\,(\boldsymbol{x}) = \sum_{i=1}^{N} C_i\, V^n\, W\left(\frac{|\boldsymbol{x}-\boldsymbol{x}_i|}{h}\right),$$

where C_i is the color of particle i, and V^n is its nominal volume. As the incompressible Navier-Stokes equations are solved the nominal volume of each particle should be the same

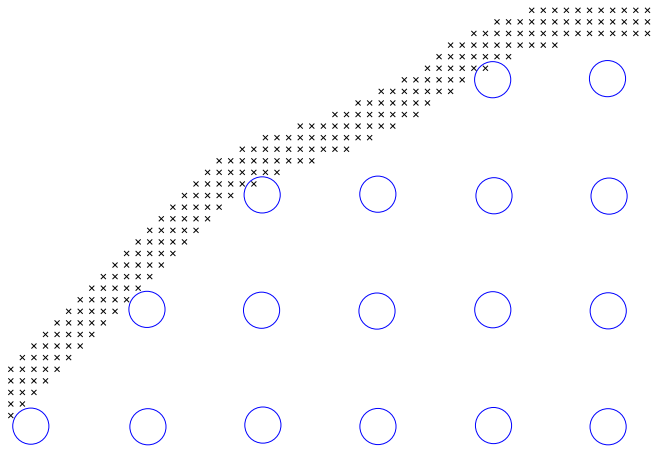

Fig. 2. Zoom in on points used to reconstruct the interface. Points shown as blue ○ are SPH particles and positions shown as black × are data points for the RBF approximation.

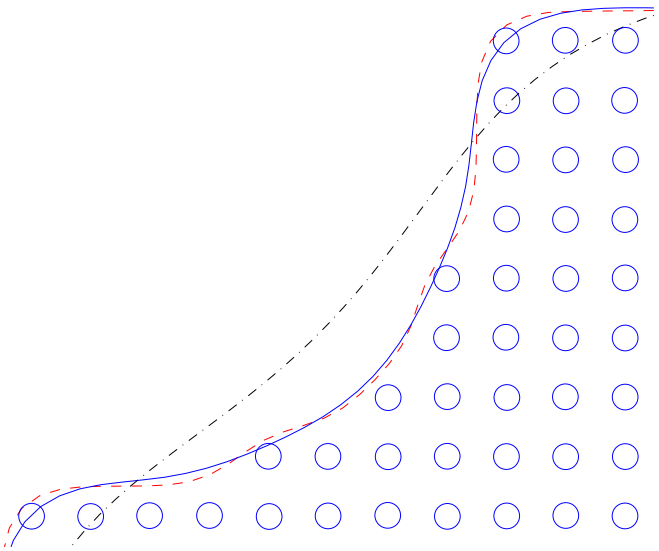

Fig. 3. Dependence of the reconstructed interface on the value of η. In the limit of $\eta \to 0_+$ (red dashed line), corresponding to pure interpolation, an interface that includes all the local features of the SPH particles (blue ○) is obtained. The largest value, $\eta = 1 - 5 \cdot 10^{-5}$ (black dash-dotted line), gives an interface that incorrectly takes a short cut in the concave region. The intermediate value, $\eta = 1 - 5 \cdot 10^{-3}$ (blue full line) represents a good trade off solution. Note that the value of η that corresponds to a given level of smoothing depends on the separation of the particles, here $h = 6.25 \cdot 10^{-5}$.

as its actual, time dependent, volume, but in practice the two differs for particles close to the interface. To avoid a spurious increase of the color function close to the interface the nominal volume, $V^n = m/\rho_0$, is used instead of the more frequent choice $V_i = m/\rho_i$.

As only the region close to the interface is of interest, only grid points having a numerical value of the color function close to C_I are retained to build the approximation upon, see Fig. 2. As the interface is defined implicitly it is important to have a reliable gradient of the approximated color function at the interface. This is why on average three data points across the interface are retained; one on the outside having a value less than C_I, one close to or at the interface, and one on the inside having a larger value. In practice, 10 times higher resolution of the evaluation grid compared to the SPH particles seems to be a suitable choice. In the tangential direction of the interface the number of data points is not as crucial, and a potential improvement is to reduce the resolution in that direction.

The approximation feature of the RBF framework is utilized at this point, and a value of the parameter η is chosen to give a good trade off between local features of the interface and smoothness of the approximation. A parameter study is shown in Fig. 3, where the reconstructed interface of a non-convex droplet is shown for three different values of η. It is clear that it is crucial to neither underestimate nor overestimate its value as it affects both the location and the local shape of the interface.

B. Surface tension force

Given the reconstructed interface the surface tension force can be evaluated. The direction of the force is normal to the interface, and the strength is proportional to its curvature, as stated in Eq. 1. Here, κ is taken to be the mean curvature in higher dimensions.

The normal vector of the interface is given by the gradient of the color function. The curvature of the surface is somewhat more complicated to evaluate, however. What we have available is the Hessian of the color function and the surface normal. These can be combined to form the expression for the mean curvature [11],

$$\kappa = \frac{\nabla C^T \, H(C) \, \nabla C - |\nabla C|^2 \, \mathrm{Trace}\left(H(C)\right)}{(d-1)\,|\nabla C|^3}, \qquad (4)$$

where d is the number of spatial dimensions.

The surface tension force is spread out over a narrow band close to the interface according to the CSF approach where a surface delta function is used [3]. The requirement that has to be fulfilled is that

$$\int_A \boldsymbol{F}_{sa}(\boldsymbol{x})\, dA = \int_V \boldsymbol{F}_{sv}(\boldsymbol{x})\, dV, \qquad (5)$$

as the width of the band approaches zero. Here, $\boldsymbol{F}_{sa}$ is the surface tension force when acting only on the interface, and $\boldsymbol{F}_{sv}$ is the corresponding volume force when acting in the narrow band. The usual expression for the surface delta function when going from $\boldsymbol{F}_{sa}$ to $\boldsymbol{F}_{sv}$ is $|\nabla C| \,/\, [C]$, where $[C]$ is the jump in the color function across the interface.

At this point we have to be careful and bear in mind that we have two different representations of the color function. First of all we have the SPH interpolation, denoted C^{SPH}, but also the corresponding RBF approximation, C^{RBF}. From the above reasoning the RBF version should have better properties for differentiation. It is not appropriate, however, to use C^{RBF} in the surface delta function, as we do not require C^{RBF} to

approach the value of the SPH color function at some distance away from the interface. Indeed, the only thing required of C^{RBF} is to give an as good as possible prediction of the direction and the curvature of the interface. In Fig. 4 both representations of the color function are shown on a line through the center of the droplet and it is clearly visible how the RBF approximation mis predicts the color function away from the interface. For this reason, C^{RBF} is used to determine the direction and strength of the surface tension, and C^{SPH} is used in the surface delta function.

An additional complication is that as only the phase within the droplet is solved for, no particles on the outside of the interface take part in the surface tension force. This can be seen in Fig. 4 where C^{SPH} approaches zero some distance away from the last SPH particle on each side. This has the consequence that Eq. 5 is not fulfilled, since the suggested surface delta function is not properly normalized. As a solution, a correction factor, χ, is introduced which accounts for the lack of the second phase. This approach can be viewed as taking the limit of the suggestion of Hu et. al. [4], where they discuss the contribution to the surface tension force on each side of an interface separating two phases having different density.

To summarize:

1) C^{RBF} is used for evaluating the interface normal and the curvature,
2) C^{SPH} is used in the surface delta function,
3) χ is introduced to account for the lack of contribution to the surface tension from the (non-existing) phase outside the droplet.

By combining this into an expression for the surface tension force, we arrive at

$$\boldsymbol{F}_s = \sigma \kappa^{\mathrm{RBF}} \frac{\nabla C^{\mathrm{RBF}}}{|\nabla C^{\mathrm{RBF}}|} \frac{\chi |\nabla C^{\mathrm{SPH}}|}{[C^{\mathrm{SPH}}]},$$

where κ^{RBF} indicates that Eq. 4 should be evaluated with C^{RBF}.

When evaluating the surface tension force at each SPH particle two different approaches to where the curvature is evaluated could be taken. The curvature could be evaluated at the interface, $C^{\mathrm{RBF}} = C_I$, and projected to the location of the particle. Alternatively, it could be evaluated at the position of the particle, in general at some small distance away from the interface. The difference between the two approaches is not expected to be too large because of the surface delta function that limits the surface tension to act only close to the interface. For this reason the second alternative is taken here since it is more straightforward to implement as it lacks the projection step.

V. Numerical results

Two test cases will be considered, both of which aims to show that the suggested surface tension evaluation behaves in a physically correct way, and that the simulations are stable even though only one phase is solved for. First, the static pressure jump over the interface of a droplet is verified. The second test case considers the time period of a droplet oscillating due to surface tension.

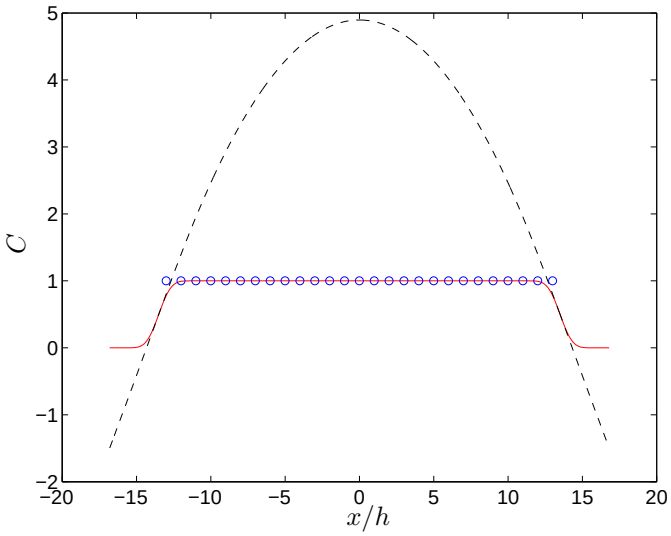

Fig. 4. Color function on a line through the center of a drop. SPH particle color (blue ○), SPH interpolation (full red line) and RBF approximation (dashed black line). The RBF approximation is only useful to predict the color level at the interface.

A. Pressure jump over an interface

The pressure jump across the interface of a static droplet scales with the droplet radius, R, according to Laplace's law,

$$\Delta p \propto \frac{1}{R} \tag{6}$$

The simulation to verify the result is set up such that the SPH particles are initially in non-equilibrium, and surface tension and viscous forces act on the droplet to form a circular shape.

The SPH particles are placed at rest in a square on a Cartesian grid, see Fig. 5 where the initial configuration is shown together with the interface of the droplet as defined by C^{RBF}. In Fig. 6 the surface tension forces can be seen as well as the local isolines of C^{RBF} running straight through the SPH particles. As expected, the surface tension acts mostly on the corners of the square. In this configuration, the effect of the smoothing parameter η in the RBF approximation is to limit the curvature at the corner somewhat, and allow more SPH particles to take part in the surface tension force. Here we use $\eta = 1 - 10^{-3}$.

After some time a circular droplet is formed and the pressure inside the droplet is higher than on the outside. Depending on the ratio of viscosity to surface tension strength, more or less oscillations occur before reaching the final circular shape. Figure 7 shows the evolution of the interface, $C^{\mathrm{RBF}}(\boldsymbol{x}) = 0.5$, over time in an overdamped setting. That is, the velocity vector of the corner particles never flips over to point away from the center. The corresponding evolution of the internal kinetic energy can be seen in Fig. 8. The values of the material

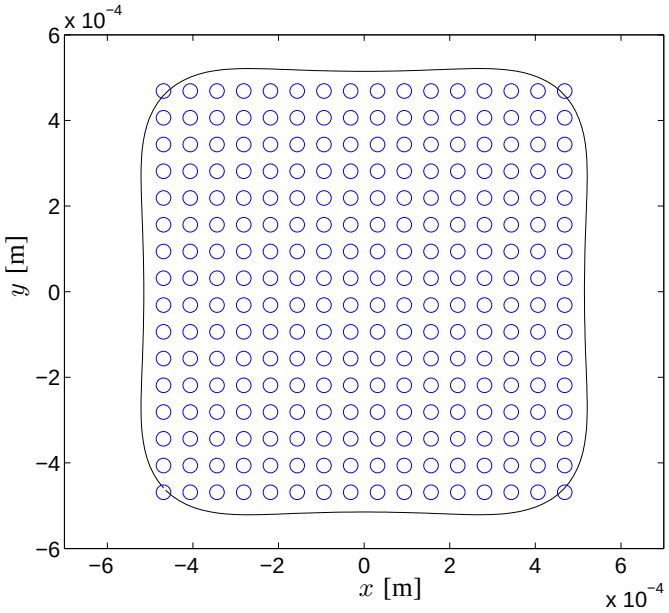

Fig. 5. Initial configuration of SPH particles (blue ○), and the interface of the droplet (full black line).

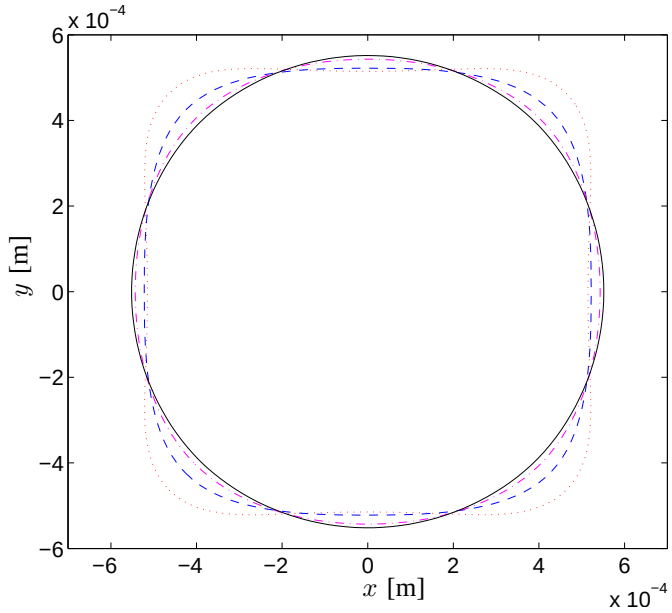

Fig. 7. Location of droplet interface at $t = 0$ s (red dotted line), $t = 7 \cdot 10^{-4}$ s (blue dashed line), $t = 14 \cdot 10^{-4}$ s (magenta dash dotted line), and $t = 21 \cdot 10^{-4}$ s (black full line) in a simulation with large viscosity.

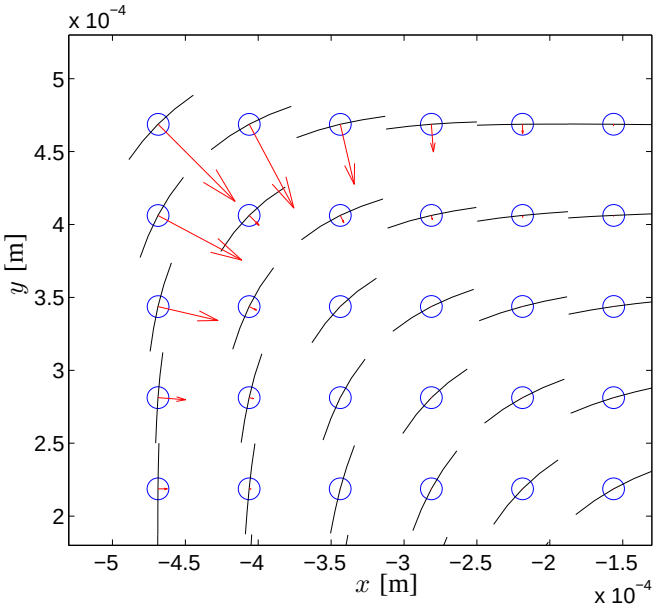

Fig. 6. Initial configuration of SPH particles (blue ○), local isolines of the color function (full black lines), and surface tension forces (red arrows).

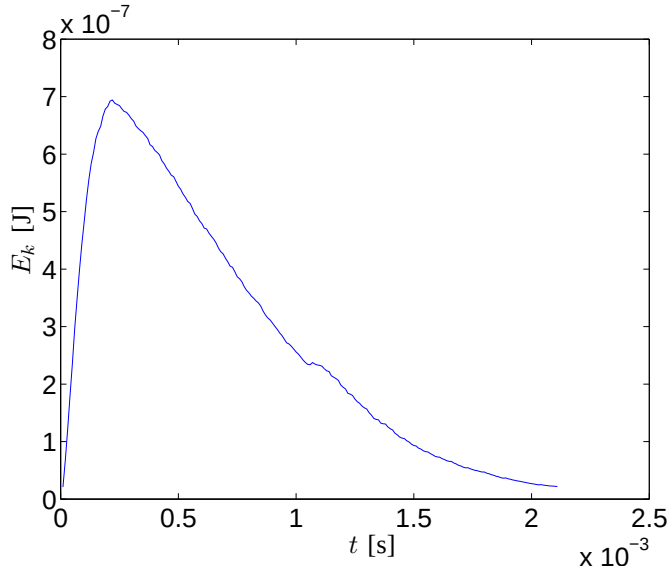

Fig. 8. Evolution of the internal kinetic energy of the droplet over time.

parameters used are $\rho = 1000$ kg/m^3, $\sigma = 0.05$ N/m, and $\mu = 0.3$ kg/s/m.

Finally, several simulations were performed for different radius of the final circular droplet. The pressure in the center of the droplet was measured when it was deemed that a steady state had been reached, and the result is shown in Fig. 9.

B. Oscillating droplet

A circular droplet of radius $R = 4.8 \cdot 10^{-3}$ m that is initially at rest and in equilibrium, is assigned the following velocity field,

$$U_x = U_0 \frac{x}{r_0} \left(1 - \frac{y^2}{r_0 r}\right) \exp\left(-\frac{r}{r_0}\right),$$

$$U_y = -U_0 \frac{y}{r_0} \left(1 - \frac{x^2}{r_0 r}\right) \exp\left(-\frac{r}{r_0}\right),$$

with $U_0 = 0.6$ m/s, and $r_0 = 5/3 \cdot 10^{-4}$ m. The values of the material parameters are in this simulation $\rho = 1000$ kg/m^3 and $\mu = 0.1$ kg/s/m.

Figure 10 shows the evolution in time of the center of gravity of the upper right quadrant of the droplet. The magnitude

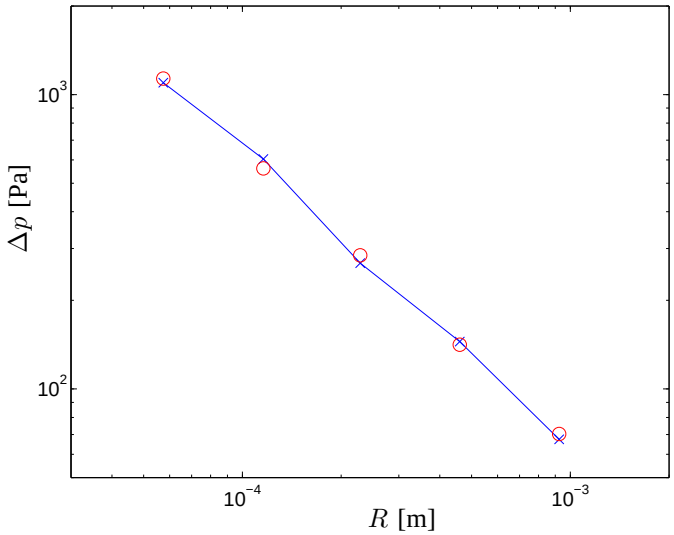

Fig. 9. Pressure jump across the interface of a droplet as a function of droplet radius. Simulation results shown as a full blue line with $\times$ markers, and analytical scaling, red $\circ$, as evaluated by Eq. 6.

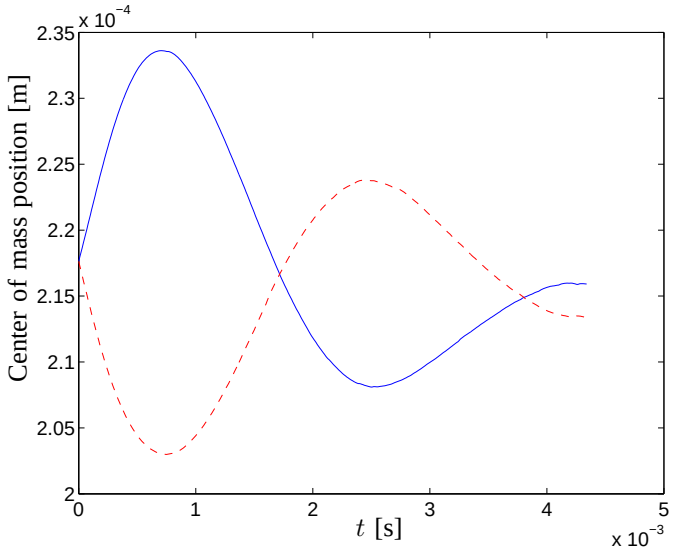

Fig. 10. Position of the center of mass of the upper right quadrant of the droplet as a function of time. Position in x shown as blue full line and the position in y as a red dashed line.

of the oscillation is decreasing with time due to viscous forces dissipating energy.

The time period of the oscillations is inversely proportional to the strength of the surface tension,

$$T \propto \frac{1}{\sqrt{\sigma}}, \tag{8}$$

or, in other words, the frequency increases with the surface tension. Fig. 11 shows the oscillation period of simulated droplets as a function of the surface tension strength. The increase in frequency is well recovered.

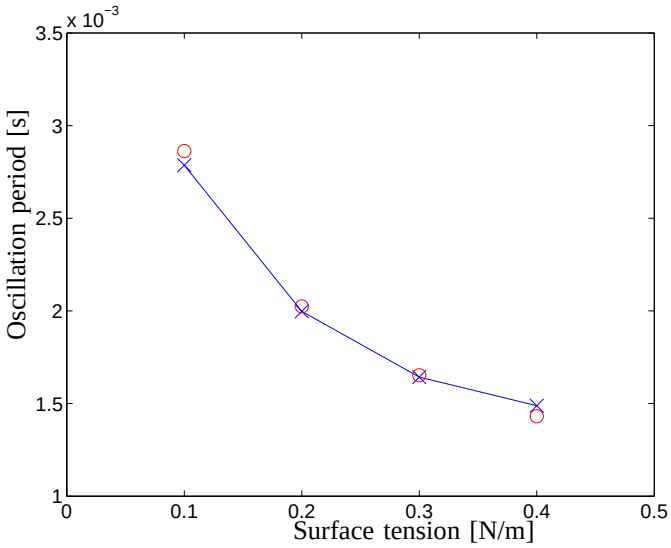

Fig. 11. Oscillation period as a function of surface tension strength. Simulation (Full blue line) and analytic scaling according to Eq. 8 (red $\circ$).

VI. Conclusions and open questions

A novel framework for reconstructing the interface separating different phases is proposed and evaluated. The main feature of the reconstruction is to provide a smooth interface that is suitable to derive a surface tension from. It is computationally more expensive than a traditional SPH formulation, but it is believed that the smoother and spatially more correlated surface tension force resulting from the new approach allows a larger time step. This would then compensate for the additional work in setting up the RBF approximation that has to be spent in each iteration of the solver. This is important not the least in free surface flows, or in situations where two fluids with large density difference are studied. We have shown that the new formulation is well suited to handle such applications.

The appropriate value of the smoothing parameter η is something that needs more investigation. As shown above, it should neither be too large nor too small. The upper limit is critical in the sense that the interface may be arbitrarily distorted to the point where it bears no resemblance with the interface provided by the SPH particles. The lower limit is not as important to keep track of, as in the worst case the original SPH interface is recovered. This would then only degrade the performance of the simulation, but the result should still be valid. For this reason a conservative approach to select the value of η should be taken in the lack of an appropriate scheme. The algorithm for placing data points for building the approximation need some fine tuning as well, as it as of today results in a very large number of grid points close to the interface. This would become an even larger issue when turning to three spatial dimensions.

It should also be noted that the proposed formulation results in a force field that is not conservative. This may, or may not be an issue depending on the situation and for how long the simulation is run. If there exists some external force, as

for example drag from a surrounding fluid, the small extra contribution to the momentum from the surface tension is most likely negligible.

ACKNOWLEDGMENT

This work has been conducted within the project Virtual PaintShop which is part of Vinnova's FFI program for sustainable production technology.

REFERENCES

[1] J. P. Morris, "Simulating surface tension with smoothed particle hydrodynamics," *International Journal for Numerical Methods in Fluids*, vol. 33, no. 3, pp. 333–353, 2000.

[2] A. Tartakovsky and P. Meakin, "Modeling of surface tension and contact angles with smoothed particle hydrodynamics," *Phys. Rev. E*, vol. 72, no. 2, p. 026301, Aug 2005.

[3] J. U. Brackbill, D. B. Kothe, and C. Zemach, "A continuum method for modeling surface tension," *Journal of Computational Physics*, vol. 100, no. 2, pp. 335 – 354, 1992.

[4] X. Y. Hu, S. Adami, and N. A. Adams, "Formulating surface tension with reproducing divergence approximation for multi-phase SPH," in *Proc. 4^{th} Int. SPHERIC Workshop*, Nantes (France), 2009, pp. 38–44.

[5] H. Wendland, *Scattered data approximation*, ser. Cambridge Monographs on Applied and Computational Mathematics. Cambridge: Cambridge University Press, 2005, vol. 17.

[6] J. P. Morris, P. J. Fox, and Y. Zhu, "Modeling low reynolds number incompressible flows using SPH," *J. Comput. Phys.*, vol. 136, no. 1, pp. 214–226, 1997.

[7] S. J. Cummins and M. Rudman, "An SPH projection method," *J. Comput. Phys.*, vol. 152, no. 2, pp. 584–607, 1999.

[8] M. D. Buhmann, "Radial basis functions," in *Acta numerica, 2000*, ser. Acta Numer. Cambridge: Cambridge Univ. Press, 2000, vol. 9, pp. 1–38.

[9] ——, *Radial basis functions: theory and implementations*, ser. Cambridge Monographs on Applied and Computational Mathematics. Cambridge: Cambridge University Press, 2003, vol. 12.

[10] S. Jakobsson, M. Patriksson, J. Rudholm, and A. Wojciechowski, "A method for simulation based optimization using radial basis functions," *Optimization and Engineering*, 2009.

[11] R. Goldman, "Curvature formulas for implicit curves and surfaces," *Computer Aided Geometric Design*, vol. 22, no. 7, pp. 632 – 658, 2005.